New experience with Allan variance: Noise analysis of accelerometers

Conference Paper · October 2017

DOI: 10.23919/KIT.2017.8109457

CITATION
1

READS
591

2 authors:

Miroslav Matejcek
General Milan Rastislav stefanik Armed Forces Academy
6 PUBLICATIONS **5** CITATIONS
SEE PROFILE

Mikulas Sostronek
General Milan Rastislav stefanik Armed Forces Academy
11 PUBLICATIONS **14** CITATIONS
SEE PROFILE

New Experience with Allan Variance

Noise analysis of accelerometers

Miroslav Matejček
Dept. of Electronics
Armed Forces Academy of gen. M. R. Štefánik
Liptovský Mikuláš, Slovakia
Miroslav.matejcek@aos.sk

Mikulaš Šostronek
Dept. of Electronics
Armed Forces Academy of gen. M. R. Štefánik
Liptovský Mikuláš, Slovakia
mikulas.sostronek@aos.sk

***Abstract* – This article deals with a noise analysis of inertial sensors, especially with accelerometers. Accelerometers and gyroscopes are inertial sensors which are parts of inertial measurement units IMUs. An inertial navigation uses outputs from three accelerometers and from three gyroscopes to positions, orientations computations. For better accuracy of navigation and guidance systems is necessary to evaluate deterministic and stochastic inertial sensors errors. Main aim of this article is to introduce new algorithm for Allan variance computation. Part of this article deals with the new practical experience with using of the Allan variance for noises and noise coefficients determination.**

Keywords – Allan variance, noise analysis, accelerometer, noise, noise coefficient

I. INTRODUCTION

Inertial sensors, gyroscopes and accelerometers are characterized by deterministic and stochastic errors. Deterministic errors are constant bias (sensor offset), scale factor errors, nonlinearity, cross axis sensitivity, and misalignment of the sensor sensitivity axis. Stochastic inertial sensors errors are noises. Allan variance (AVAR), power spectral density (PSD), and autocolerration function (ACF) are the method for stochastic errors computation and evaluation [2]. AVAR uses time averaging technique and PSD uses frequency averaging technique for their computation.

Allan variance (AVAR) is the method characterized by its simplicity. Allan variance method benefits are good visibility and visualization of sensors noises. Allan variance evaluates characteristic noises, and noise coefficients of accelerometers (gyroscopes) which are quantization noise, sinusoidal noises, exponentially correlated (Markov) noise, velocity random walk VRW (Angle Random Walk ARW), bias instability BI, acceleration random walk AccRW (Rate Random Walk RRW), acceleration ramp AccR (Rate Ramp RR) [1], [2].

Allan variance method is based on the computation of root mean square random drift error as a function of average time [1], [2].

AVAR in the time domain according to (2) is used for analysis of sensor output as a function of interval τ. AVAR is related to total power output of random signal after it passed through band pass filter with specific transfer function. In this way, when $\tau = m\tau_0$ is changed, transfer function of the band pass filter is also changed and the different stochastic errors can be estimated.

$$\sigma^2(\tau) = 4\int_0^{\infty} S_0(f)\frac{\sin^4(\pi f\tau)}{(\pi f\tau)^2} \qquad (1)$$

Where S_0 is PSD of the sensor output signal, f is frequency.

The log-log plot of Allan deviation (ADEV) (square root of AVAR) is used for the practical noises determination according to Figure 1.

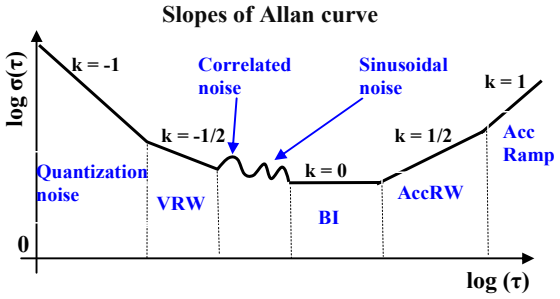

Figure 1. Allan Variance curve

According to cluster averaging techniques [1] nonoverlapped AVAR, not fully overlapping AVAR, fully overlapping AVAR, total variance and modified total variance [1] could be used for the AVAR computation. Figure 2 explains nonoverlapped cluster averaging techniques. There N measurement with sample time τ_0 is divided into the M clusters. Every cluster has length (cluster time) $\tau_m = m\tau_0$ and the mean value of every cluster data is called the cluster sample.

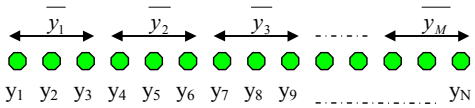

Figure 2. Nonoverlapped cluster averaging technique

AVAR is computed according to equation [1]

$$\sigma_y^2(\tau) = \frac{1}{2(M-1)}\sum_{j=1}^{M-1}\left[\bar{y}_{j+1} - \bar{y}_j\right]^2. \qquad (2)$$

Where M is the number of cluster samples ($\bar{y}_k$). Average of the clusters is expressed according to following expression

$$\bar{y}_k(m) = \frac{1}{m}\sum_{i=1}^{m} y_{(k-1)d+1} \tag{3}$$

where $k = 0, 1,...M$. The cluster time is $m \leq N/2$. The step d for nonoverlapped cluster sampling techniques is equal to m [1]. The number of clusters M depends on the Allan variance method according to expression [1]

$$M = \left[\frac{N}{m}\right]\frac{m}{d} - \frac{m}{d} + 1 \tag{4}$$

Accuracy of AVAR is defined by the percentage error I and following equation

$$I = \frac{1}{\sqrt{2(M-1)}} \tag{5}$$

From the I value are computed confidence intervals for 1 σ (68 %) according to equations

$$\begin{aligned} \sigma_{\max}(\tau) &= \sigma(\tau)(1+I), \\ \sigma_{\min}(\tau) &= \sigma(\tau)(1-I). \end{aligned} \tag{6}$$

Nonoverlapped method for AVAR computation was chosen because its simplicity, short computation times. Disadvantage of nonoverlapped method is relative higher error level defined according to (5) and (6).

Proposal of nonoverlapped method script is created in program MATLAB. Main part of script mentioned below consist of g (gravity vector) computation [10], computation of integer dividers from N, cluster sampling section and averaging part and plotting section.

```
% NON OVERLAPPED ALLAN VARIANCE
K1X = 0.51489  % DLU690BI scale factor V/g
g_0standard = 9.80665; % standard g value
L = 49.066485633; % latitude
l = 19.591090679; % longitude
h = 690; % altitude
R0 = 6371000; % Earth radius (mean value)
g_0 = 9.780318*(1+5.3024e-3*sin(L)^2-5.9e-
6*sin(2*L)^2); g value without h influence
g = g_0/(1+h/R0)^2 % overall g value
N =720000 ; % measurement number
number=N;
facnum = factor(number);% prime factor calcul
uf = unique(facnum);% sort without repetition
hf = histc(facnum,uf);% histogram count
vec = (uf(1)).^(0:hf(1));
for i=2:length(uf);
    fac = uf(i);
    x = fac.^(0:hf(i));
    vec = kron(vec,x); % Kronecker tensor
end
div = sort(vec)  % sort (ascending order)
m = length(div); % integer divisors number
C1 = A(1:N,3); % load measurements
B1 = g.*C1./K1X; % units conversion
for i=1:1
Y = zeros(div(i),N/div(i)); % zeros array
Y = reshape(B1,div(i),N/div(i));% reshape B1
avarY = zeros(1,N/div(i)-1); % zeros array
for j=1:N/div(i)-1
avarY(1,j) = (Y(j+1)- Y(j))^2;
end
avar1 = (0.5*sum(avarY))/(N/div(i)-1);
adev(1,i) = sqrt(avar1);
end
for i=2:length(div)-1
Y = zeros(div(i),N/div(i)); % zeros array
Y = reshape(B1,div(i),N/div(i)); reshape B1
avarY = zeros(1,N/div(i)-1); % zeros array
Yavg = mean(Y); % cluster mean values
for j=1:N/div(i)-1
avarY(1,j) = (Yavg(j+1)- Yavg(j))^2;
end
avar1 = (0.5*sum(avarY))/(N/div(i)-1); % AVAR
adev(1,i) = sqrt(avar1); % ADEV values
end
div_interval = div(1:length(div)-1); % τ(tau)
loglog(div_interval/100,adev,'r') % plotting
title('ADEV DLU690BI') % add graph title
xlabel('time [seconds]') % add x-axis label
ylabel('ADEV [ms^-^2]') % add x-axis label
hold on
grid on
```

After ADEV computation and plotting Allan curves they are approximated with help of approximation function. Approximation functions are depicted on Figure 1 lines with characteristic slopes -1, -0.5, 0, +0.5, +1. Different noise types or noise coefficients could be determined from specific τ regions and with help of approximation functions.

II. Practical Measurements

MEMS accelerometers ADXL326 (Analog Devices), FXLN8372 (NXP Semiconductors), linear accelerometer DLU690BI, accelerometer of IMU ADIS 16354 (Analog Devices) were used for the next measurements. Measurements and noise evaluation for accelerometers ADXL326, FXLN8372 were realized for N=2.7×10^6 samples, for DLU690BI 7.2×10^5 samples, and for ADIS16354 2.7×10^6 samples with sampling frequency 100 Hz. Noise and noise determination principle is explained in Figures 2 and 3. ADEV could be computed from one measurement, but for better accuracy of noise determination, four measurement Adev(1 up to 4) were realized. From Adev(1up to 4) were computed mean values ADEV X, Y, Z (mean).

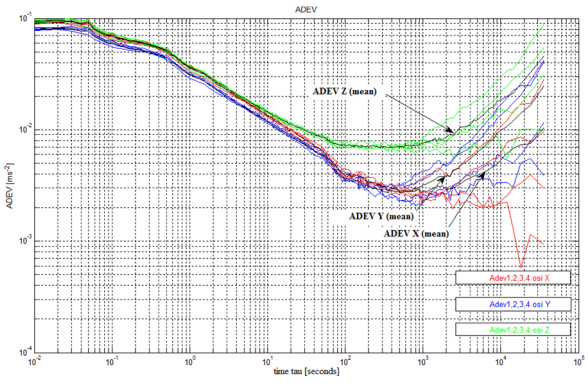

Figure 3. ADEV computation of accelerometer ADXL326

Approximation lines with specific slopes [1] (- 0.5, 0, +0.5, +1) were used on curves ADEV X, Y, Z (mean) as in figure 4.

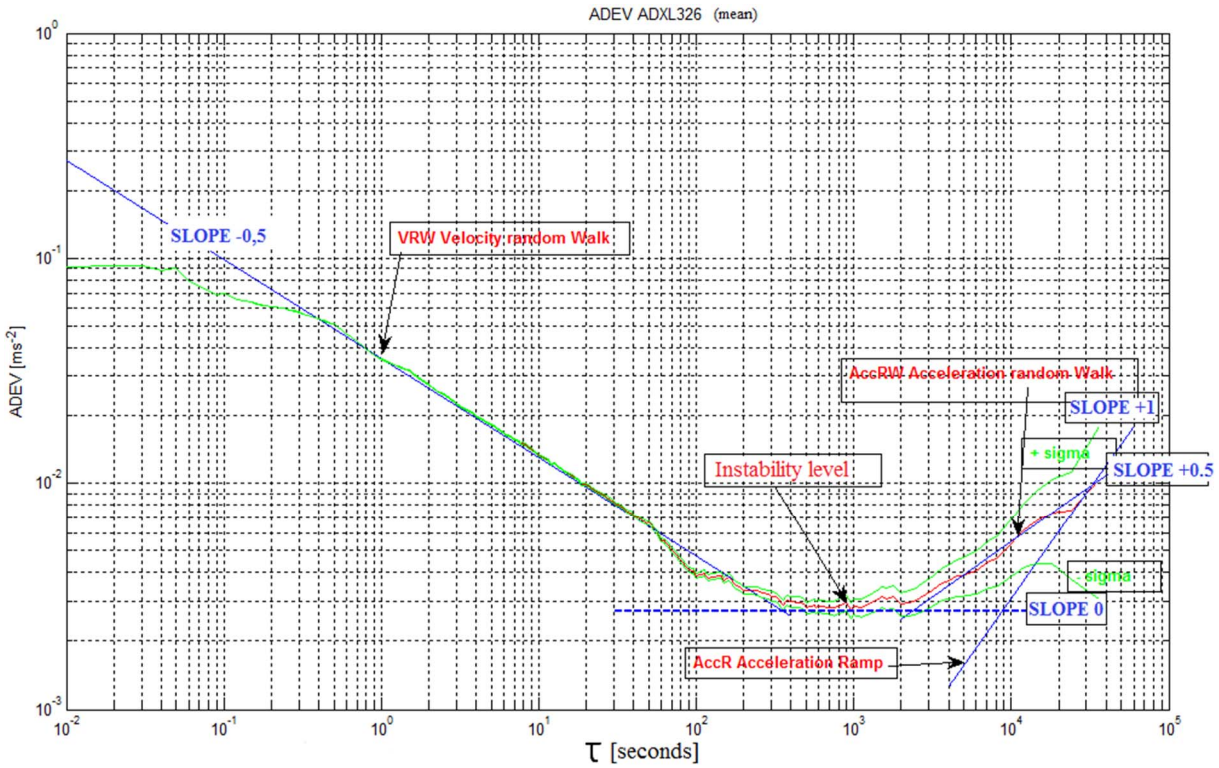

Figure 4. Prinsiple of noise nalysis for the accelerometer ADXL326

Velocity Random walk (VRW) is expressed by line with slope -0.5. VRW coefficient N_{ABS} is determined from the line -0.5 at τ=1 sec. True coefficient value (listed in datasheets) is computed N_{TRUE} =60× N_{ABS} [1]. VRW is high frequency noise. Its correlation time is shorter than value of sample time. ARW is a white noise at the sensor output.

Bias instability (BI) is characterized by the line with slope 0. BI coefficient B_{ABS} is determined from minimal ADEV values and it is divided by the value 0.664 [3], [4], [5], [6]. Value BI which is in datasheets is B_{TRUE} = 3600× B_{ABS} [1]. Source of bias instability is in the low frequency flicker noise of sensor electronic components.

Exponentially correlated (Markov) noise is characterized by exponential decaying function with finite correlation time [3]. Noise amplitude is determined from the characteristic wider peak on ADEV in Fig. 1 and it is divided by number $0.437\times(T_C)^{1/2}$, where correlation time T_C=1.89τ [3], [4].

Sinusoidal noise is generated by high or low frequency inner (in sensor structure) or outer sources. Sinusoidal noise amplitude is evaluated from the first peak of sinusoidal curve of Allan curve (Figure. 1) and it is divided by factor 0.725 [1], [3].

Acceleration random walk AccRW is characterized by the line with slope +0.5. AccRW coefficient K_{ABS} is computed from the line with slope 0.5 at τ=*3* sec. Real values is defined as K_{REAL}= 3600×60×K_{ABS} [1]. AccRW is the limit case of exponentially correlated noise with very long correlation time [3], [4]. Source of this noise is unknown yet.

Acceleration ramp (AccR) is determined by the line with slope +1. AccR coefficient R is estimated from ADEV or region with slope +1 at $\tau=2^{1/2}$. AccR is a noise with more deterministic character than the fully random process. The value of the R_{ABS} is estimated from Allan curve or region with slope +1 at $\tau=2^{1/2}$. Real (datasheet) value R_{TRUE}=3600²× R_{ABS}.

Accuracy of noise coefficients estimation is computed according (5), (6) and for ADXL 326 (coefficients *N, B, K, R*) percentage errors is 0.26 *%*, 8.22 *%*, 29.7 *%* a 19.5 *%*. Intervals (± σ) are in the Figure 4 (green curves). Real noise coefficient values are listed in Table 1. If noises are statistical independent, overall noise values expressed by AVAR is determined according to follow equation [1],

$$\sigma^2_{Total}(\tau)=\frac{3Q^2}{\tau^2}+\frac{N^2}{\tau}+\frac{2B^2\ln 2}{\pi}+\frac{K^2\tau}{3}+\frac{R^2\tau^2}{2} \quad (7)$$

III. Evaluation of the Allan Variance Results

Results of AVAR computation are listed in Table 1. Low cost accelerometers ADXL326 and FXLN8372 have approximately the same values VRW (from value 2 to 3 [m/s/h$^{1/2}$]). Values B_{REAL} (for *X, Y* axes), K_{REAL}, R_{REAL} of AXL326 are almost two times lower than for FXLN8372. The smallest values of BI coefficient B_{REAL}, and VRW coefficient N_{REAL} was computed for DLU690BI B_{REAL} = 1.51 m/s/h, N_{REAL} = 5.1×10^{-2} m/s/h$^{1/2}$. The second the best values of VRW, BI coefficient were computed for ADIS16354 accelerometer, where B_{REAL} values are from 2.8 to 3.6 m/s/h (depends on the axis) and N_{REAL} is from 1.17×10^{-1} to 0.126×10^{-1} m/s/h$^{1/2}$.

TABLE I. REAL NOISE COEFFICIENT VALUES

Sensor	N_{REAL} [m/s/h$^{1/2}$]	B_{REAL} [m/s/h]	K_{REAL} [m/s/h$^{3/2}$]	R_{REAL} [m/s/h^2]
ADXL326 X, Y, Z	2.16 ± 0.26 %	14.83 ± 8.2 %	22.2 ± 29.7 %	6.73 ± 19.5 %
	1.92 ± 0.26 %	14.74 ± 5 %	35.89 ± 29.7 %	16 ± 19.5 %
	2.34± 0.26 %	37.32 ± 5.28 %	74 ± 29.7 %	30.9 ± 19.5 %
FXLN8372 X, Y, Z	2.94 ± 0.26 %	33 ± 5 %	55.1 ± 29.7 %	15.83 ± 19.5 %
	2.94 ± 0.26 %	30.3 ± 6.27 %	45.5 ± 29.7 %	15.47 ± 19.5 %
	2.04 ± 0.26 %	29.81 ± 4.48 %	40.7 ± 29.7 %	14.56 ± 19.5 %
DLU690BI	5.1×10^{-2} ± 0.83 %	1.51 ± 3.23 %	22.57± 29.7 %	unspecified
ADIS16354 X, Y, Z	$1.26*10^{-1}$ ± 0.44 %	3.3 ± 1.96 %	15.7 ± 59.6 %	14.56 ± 34.9 %
	$1.17*10^{-1}$ ± 0.44 %	3.6 ± 2.28 %	11.1 ± 59.6 %	10.92 ± 34.9 %
	$1.17*10^{-1}$ ± 0.44 %	2.8 ± 2.8 %	11.1 ± 59.6 %	10.92 ± 34.9 %

Datasheet values [5] for ADIS16354 VRW 0.135 ms^{-1}h$^{-1/2}$ and estimated values are quite lower (from 0.117 ms^{-1}h$^{-1/2}$ to 0.126 ms^{-1}h$^{-1/2}$). BI from ADIS16354 datasheet is 4.9×10^{-4} ms^{-2}, and from minimal Allan curve value were estimated real values 6.1×10^{-4} (*X*-axis), 6.65×10^{-4} (*Y*-axis), 5.2×10^{-4} ms^{-2} (*Z*-axis).

IV. CONCLUSION

AVAR is the simple way for noise analysis of inertial sensors noise performance. AVAR advantages are simplicity and exactness of noise coefficient determination. Nonoverlapped method of AVAR (ADEV) computation uses nonoverlapping cluster sampling techniques. This method is characterized by short computation times, but from the another hand its computation errors is higher than computation errors of not fully overlapped (or fully overlapped) method. Proposed MATLAB script computation time for $N=2.7\times10^6$ measurements was approximately 4 seconds for one axis. Measurements and evaluation noise performance of selected accelerometers determined their qualities. Low cost MEMS accelerometers ADXL326, FXLN8372 have worse noise features, thanks to MEMS technology without additional filtering and noise compensation. The next disadvantages of a number of MEMS sensors are a small value of scale factor (sensitivity), a small weight value of sensing element with combination with sensor structure defects [8], [9]. ADIS16354 accelerometer noise features are better, thanks to Barlett Window FIR filter for additional noise reduction. The best values of VRW and BI coefficients were computed for linear accelerometer DLU690BI. ADEV computation errors grow rapidly for all measurements, according to (5) when *M* is decreased.

REFERENCES

[1] Jintao Li and Jeancheng Fang, "Not Fully Overlapping Allan Variance and Total Variance for Inertial Sensor Stochastic Error Analysis," IEEE Transaction and Measurement, vol. 62, No. 10, pp. 2659-2672, 2013.

[2] M. Soták, "Estimation of stochastic coefficient of inertial sensors," Science and Military, Armed Forces Academy, 2008.

[3] IEEE Standard specification format guide and test procedure for single axis interferometric fiber optic gyros, IEEE std. 952^{TM}-1997, 2008.

[4] IEEE Standard specification format guide and test procedure for single axis laser gyros, IEEE std. 647^{TM}-2006, 2006.

[5] Analog Devices Inc., High Precision 3-axis Inertial sensor ADIS16354, available online:
http://www.analog.com/media/en/technical-documentation/obsolete-data-sheets/ADIS16354.pdf.

[6] V. KŘIVÁNEK, "Application LAMDA algorithm for Fault Detection and Isolation," In: 14th International Conference on Mechatronics, MECHATRONIKA 2011, 2011, p. 46-51.

[7] K. Draganová, F. Kmec, J. Blažek, D. Praslička, J. Hudák, and M. Laššák, "Noise Analysis of Magnetic Sensors Using Allan Variance," in Proceedings 15th Czech and Slovak conference on Magnetism, Košice. Slovakia, 2013, p. 394-395.

[8] M. Soták, M. Sopata, R. Bréda, and Ľ. Váci, Integration of navigation systems, Košice: R. Bréda, 2006.

[9] T. KLIMENT, D. PRASLIČKA, K. DRAGANOVÁ, J. BLAŽEK, "Gradient methodology for 3-axis magnetometer scalar calibration ", In: Journal of Electrical Engineering: Magnetic Measurement 2015.Bratislava> STU, 2015 year. 66 Num.7 (2015), p.157-160, ISSN1335-3632.

[10] TITTERTON D., J. Weston. 2004. *Strapdown Inertial Navigation Technology*. Second edition: The American Institute of Aeronautics and Astronautics, 2004.